

Critical Role of Imaging in the Neurosurgical and Radiotherapeutic Management of Brain Tumors¹

Lily L. Wang, MBBS, MPH

James L. Leach, MD

John C. Breneman, MD

Christopher M. McPherson, MD

Mary F. Gaskill-Shipley, MD

Abbreviations: ADC = apparent diffusion coefficient, AF = arcuate fasciculus, BOLD = blood oxygen level-dependent, CBV = cerebral blood volume, CNS = central nervous system, CST = corticospinal tract, CTV = clinical target volume, DSC = dynamic susceptibility contrast, DTI = diffusion tensor imaging, DW = diffusion-weighted, ESM = electrocortical stimulation mapping, FLAIR = fluid-attenuated inversion recovery, GBM = glioblastoma multiforme, GTV = gross tumor volume, NAA = *N*-acetylaspartate, TE = echo time

RadioGraphics 2014; 34:702–721

Published online 10.1148/rg.343130156

Content Codes: **CT** **MR** **NR** **OI**

¹From the Departments of Radiology (L.L.W., J.L.L., M.F.G.S.), Radiation Oncology (J.C.B.), and Neurosurgery (C.M.M.), University of Cincinnati College of Medicine, 234 Goodman St, Cincinnati, OH 45267-0761; Brain Tumor Center at the UC Neuroscience Institute and UC Cancer Institute (L.L.W., J.L.L., J.C.B., C.M.M., M.F.G.S.); and Departments of Radiology (J.L.L.) and Radiation Oncology (J.C.B.), Cincinnati Children's Hospital Medical Center, Cincinnati, Ohio. Presented as an education exhibit at the 2012 RSNA Annual Meeting. Received June 11, 2013; revision requested September 4 and received December 30; accepted January 22, 2014. All authors have no financial relationships to disclose. **Address correspondence to** M.F.G.S. (e-mail: mary.gaskill-shipley@uchealth.com).

TEACHING POINTS

See last page

Introduction

Imaging has played an increasingly crucial role in guiding neurosurgical and radiotherapeutic management of brain tumors, especially since the development of computed tomography (CT) and magnetic resonance (MR) imaging. In recent years, the evolution of new imaging techniques, including diffusion-weighted (DW) imaging, perfusion MR imaging, spectroscopy, functional MR imaging, and diffusion tensor imaging (DTI), has not only improved the preoperative assessment of tumors, but has also expanded surgical approaches, aided in radiation treatment planning, and become a critical tool in evaluating therapeutic outcomes. The 2012 Oncodiagnosis Panel presented an overview of how comprehensive MR imaging plays an integral role in the multidisciplinary approach to brain tumors. In this article, we discuss how the use of a variety of imaging techniques can aid in the diagnosis and appropriate treatment of intracranial lesions.

Preoperative Assessment of Brain Tumors

In the past 30 years, MR imaging has become the primary imaging modality in the evaluation of brain tumors. Conventional sequences provide an immense amount of data, including the location, signal intensities, and enhancement characteristics of mass lesions. These images typically suffice for accurate diagnosis and treatment planning. In many patients, however, advanced imaging techniques can yield further refinement of the differential diagnosis or management plan (1,2). In conjunction with conventional sequences, an integrated approach can now include DW imaging, MR spectroscopy, perfusion MR imaging, DTI, and functional MR imaging.

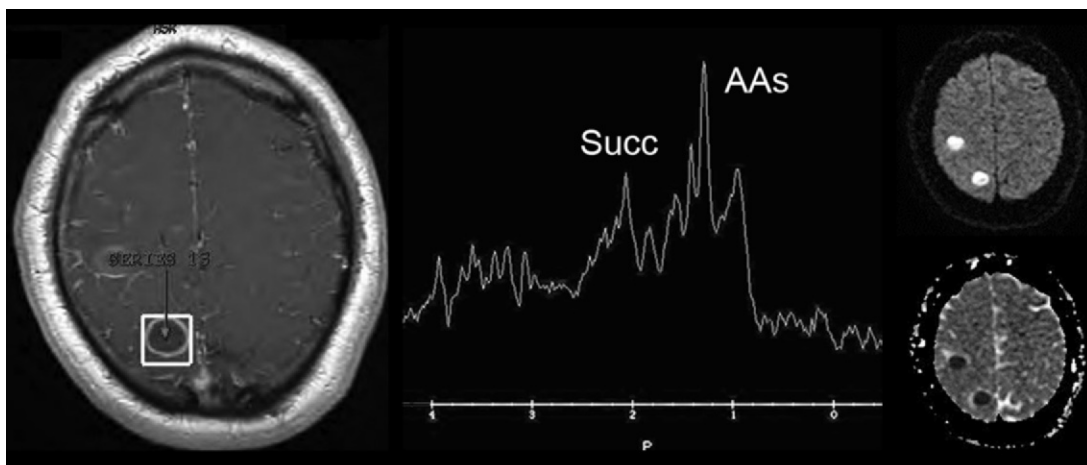


Figure 1. Pyogenic abscess in a 35-year-old man with altered mental status. T1-weighted MR image obtained after contrast material administration (left) shows a ring-enhancing lesion (box) in the right parietal lobe, which at another institution was thought to be a metastatic lesion. MR spectroscopic image (echo time [TE] = 35 msec) (middle) shows no elevation of the choline level, with elevated levels of succinate (*Succ*) and amino acids (*AAs*), possibly including alanine, findings that characterize abscess. DW image (top right) and ADC map (bottom right) show two lesions with restricted diffusion in their central nonenhancing portions.

DW Imaging

DW imaging is an echo-planar technique that maps the rate at which extracellular water molecules diffuse through tissue (3). The mobility of water molecules at the molecular level is determined by both the cellularity of the environment and thermal agitation. The intensity of each voxel on a DW image reflects an estimate of the rate of water diffusion. Within fluid (eg, cerebrospinal fluid), there is no impedance to the flow of water molecules and therefore no diffusion restriction. In brain tissue, however, rates of diffusion are slower because of normal parenchymal components that hinder the movement of water. Pathologic processes can further restrict water diffusion, thereby reducing the apparent diffusion coefficient (ADC) (4).

DW imaging is perhaps most commonly used in the detection of acute infarction, in which diffusion restriction has a complex cause but is believed to be partially due to the rapid onset of cytotoxic edema (5). This changes the intracellular-to-extracellular water ratio and reduces the volume of the extracellular spaces, resulting in diffusion restriction.

In recent years, the use of DW imaging to evaluate intracranial masses has increased in terms of (for example) the differentiation of ring-enhancing or necrotic tumors from abscesses. The central cavities of necrotic tumors typically have fluid characteristics and do not demonstrate diffusion restriction. However, abscess cavities do exhibit significant reduction in ADC values (Fig 1) (6).

The presence of diffusion restriction may provide clues to identifying the tumor type; however,

there is considerable overlap among the various histologic profiles (4,7). Compared with normal brain parenchyma, tumors with high cellularity often have reduced ADC values or greater diffusion restriction caused by decreased extracellular spaces (8). Up to 90% of primary central nervous system (CNS) lymphomas, which are typically homogeneous hypercellular tumors, demonstrate diffusion restriction (9). However, this finding is not specific, since other cellular tumors, including glioblastoma multiforme (GBM) and meningioma, may also exhibit diffusion restriction (10,11).

Perfusion MR Imaging

There are three main perfusion MR imaging techniques that are used to evaluate the hemodynamics of brain tumors. Two methods, dynamic susceptibility contrast (DSC) perfusion and dynamic contrast material-enhanced perfusion, require the intravenous administration of gadolinium-based contrast material. The third method, arterial spin labeling, makes use of magnetically labeled water in the blood rather than gadolinium (12). DSC perfusion is currently the most widely used technique in both stroke and tumor imaging. However, the use of dynamic contrast-enhanced imaging to assess the capillary permeability of brain tumors is increasing rapidly (13).

DSC perfusion relies on a negative enhancement technique that makes use of the T2 and T2* effects of contrast material (14). High concentrations of gadolinium cause T2 shortening in adjacent tissues. The degree of dephasing and resulting signal change that occur during bolus injection of gadolinium-based contrast material

can be measured and plotted as a time–signal intensity curve, with the area under the curve being proportional to the cerebral blood volume (CBV). This is not an absolute value; CBV is expressed as a relative measurement that allows the lesion to be compared with the contralateral normal white matter or corresponding structure (15). DSC perfusion is a robust technique that is available on most commercial MR imagers, but it does have limitations. Given that it is often performed as a gradient sequence to enhance the detection of T2 signal changes, DSC perfusion is adversely affected by hemorrhage or postsurgical changes that cause susceptibility artifact. In addition, relative CBV measurements can be incorrectly calculated in tumors with significant capillary permeability. The use of dynamic contrast-enhanced T1-weighted perfusion imaging with calculation of K_{trans} values can provide better assessment of permeability and vascular leakiness and may offset some of the limitations of the DSC technique.

Different tumor types and grades differ in their perfusion characteristics. For example, a strong correlation is found between the grade of astrocytoma and relative CBV measurements (16). As the tumor grade worsens, the relative CBV ratios typically increase. However, there can be significant overlap between the grades and considerable variability depending on histologic type. Interestingly, oligodendrogiomas—even those of low grade—tend to have significantly elevated relative CBVs (17), likely owing to the extensive angiogenesis and dense capillary networks that characterize these tumors.

Differentiating primary CNS lymphoma from other neoplasms is important for the radiologist because surgical resection of lymphoma is contraindicated. If lymphoma is suspected at preoperative imaging, the surgeon will alter the approach, performing a biopsy rather than excision. In addition to the frequent presence of diffusion restriction, lymphoma can have a characteristic perfusion pattern (Fig 2). **Compared with GBM, lymphomas typically have lower relative CBV ratios due to differences in tumor vascularity.** Although it is not a specific finding, lymphomas often demonstrate increased signal relative to baseline in the recovery phase due to contrast material leakage within the interstitial space (13,18,19). Perfusion MR imaging can be helpful in differentiating neoplasms from other intracranial disease entities that can mimic tumors at conventional imaging. Subacute enhancing infarcts, abscesses, and other inflammatory processes usually have decreased relative CBV ratios. Acute enhancing multiple sclerosis plaques may demonstrate mild elevation of rela-

tive CBV, although not typically to the same extent as enhancing tumors (20,21).

MR Spectroscopy

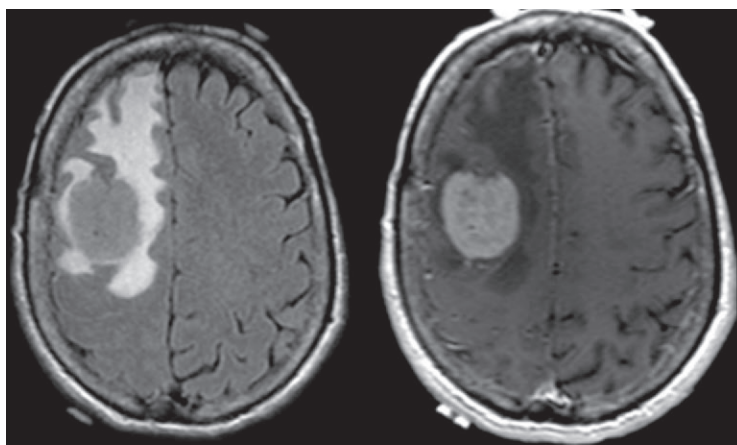
MR spectroscopy provides analysis of different metabolites within the brain and can be useful in the initial diagnosis of brain tumors, as well as in directing biopsy, grading, and treatment assessment (1,22–24). Although a full discussion of MR spectroscopy is beyond the scope of this article, correct interpretation of MR spectroscopic findings relies on a thorough knowledge of the techniques used.

MR spectroscopy can be performed with a single-voxel technique, in which a solitary spectrum is produced for a volume of tissue, or with a multivoxel technique, in which a larger volume of tissue is evaluated and then divided into smaller sections. The single-voxel technique is easier to perform, especially in posttherapy patients. However, the multivoxel technique allows evaluation of specific areas of a lesion, which in turn may help direct therapy or determine the optimal site for biopsy (25).

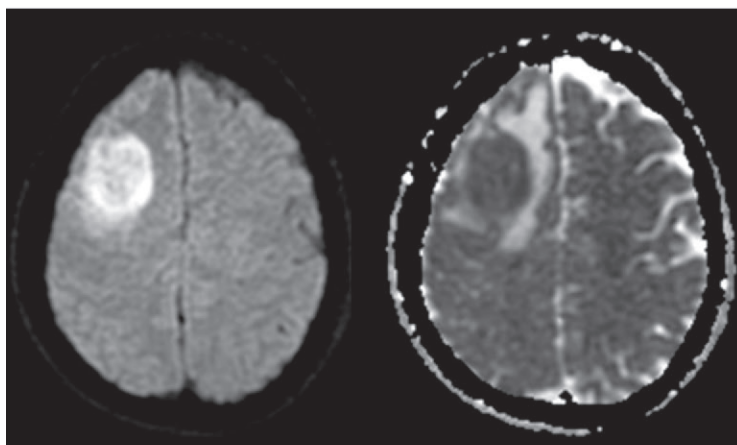
The major metabolites evaluated in proton MR spectroscopy include *N*-acetylaspartate (NAA) (normal neuronal marker), choline (cell membrane marker), creatine (energy marker), lactate (metabolic acidosis), and lipids (tissue breakdown and cell death). The spectral patterns of intracranial neoplasms vary significantly because of the differences in tumor types and grades. However, most CNS tumors manifest with elevation of the choline-creatinine and choline-NAA ratios caused by increases in cellularity (elevation of choline) and relative decreases in normal neurons (reduction of NAA) (26). Although choline-creatine and choline-NAA ratios are elevated in high-grade gliomas, there is significant overlap between the different grades. Lactate-lipid peaks are not present in normal brain tissue but will be seen in areas of necrosis.

Primary CNS lymphomas typically manifest with significantly elevated choline-creatine and choline-NAA ratios. In addition, lactate-lipid peaks are present in up to 90% of cases (9) and often appear disproportionate to the degree of necrosis seen (Fig 2d).

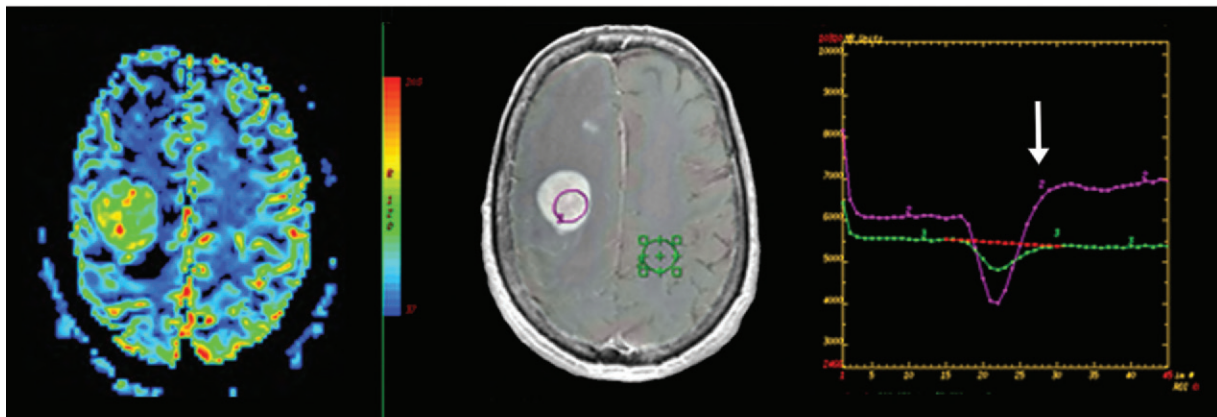
Although MR spectroscopy can be helpful in differentiating tumors from other intracranial mass lesions such as abscesses (27), other lesions can simulate tumors. Acute demyelinating plaques can manifest with significantly elevated choline-creatine and reduced NAA-creatine ratios that mimic tumor MR spectroscopic signatures. Therefore, careful analysis of the conventional images and correlation with the clinical presentation are important in these cases.



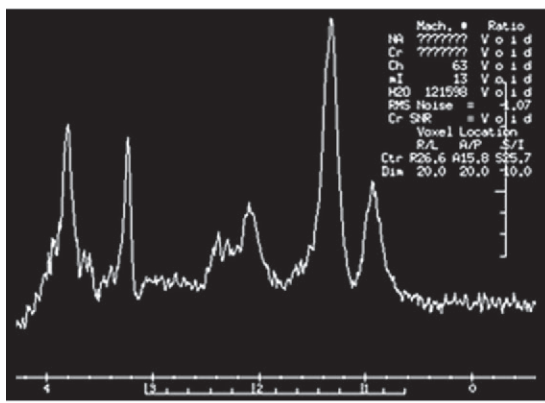
a.



b.



c.



d.

Figure 2. Primary CNS lymphoma in a 63-year-old woman who presented with new-onset headache and seizure. **(a)** T2-weighted fluid-attenuated inversion recovery (FLAIR) (left) and gadolinium-enhanced T1-weighted (right) MR images demonstrate a T2-hyperintense, homogeneously enhancing lesion with adjacent edema. **(b)** DW image (left), with accompanying ADC map (right), demonstrates restricted diffusion within the enhancing lesion. **(c)** DSC perfusion MR image (left), conventional MR image (middle), and time–signal intensity graph (right) demonstrate hyperperfusion within the area of enhancement. On the perfusion color map, the lesion is green, and red represents increased CBV compared with the contralateral white matter (blue). Arrow on graph = overshoot in the recovery phase caused by contrast material leakage into the interstitial space, a finding that is characteristic of lymphoma. **(d)** MR spectroscopic image (TE = 35 msec) demonstrates an elevated choline peak and a prominent lactate-lipid doublet. Long-TE MR spectroscopy helped confirm the presence of a small lipid peak.

Functional MR Imaging and DTI

The extent of resection, a major factor that affects long-term survival in brain tumor patients (28,29), can largely be determined on the basis of the proximity of the lesion to eloquent brain regions (30). Preoperative imaging techniques that are increasingly being used to outline eloquent brain regions prior to resection include functional MR imaging and DTI (31). Although further validation is needed, these two techniques, especially in combination, allow comprehensive evaluation of at-risk brain regions and can help guide surgical therapy (31).

Functional MR imaging is based on the blood oxygen level-dependent (BOLD) contrast effect and physiologic neurovascular coupling (32,33). When a certain cognitive task is being performed, activation of specific brain regions and networks of brain regions increases, which in turn leads to related regional increases in cerebral blood flow. This increase (neurovascular coupling) results in a relative excess of oxyhemoglobin in the regional vascular bed. Sequences used for functional MR imaging (typically echo-planar T2* gradient-echo sequences) are sensitive to changes in hemoglobin oxygenation states with greater concentrations of diamagnetic oxyhemoglobin than paramagnetic deoxyhemoglobin, resulting in increased relative MR signal. With application of these sensitive MR imaging techniques during a cognitive task, changes that affect MR signal secondarily reflecting regional cerebral neuronal activity can be detected (34). Because these signal changes are small, repeated measurements of the neuronal activity-related BOLD contrast effect are needed during a cognitive task to enhance detectability. Although many techniques have been described, a blocked functional MR imaging paradigm design is typically used for clinical work. In this design, alternating periods of an active task (the functional domain of concern, ie, the sensorimotor, language, or vision domain) and a control task (a cognitively matched task or rest) are performed over a 4–6-minute span (the functional MR imaging paradigm). Task and control periods are then statistically compared on a voxel-by-voxel basis with use of a variety of techniques to identify task-related signal changes (35). Multiple paradigms for assessing different cognitive domains can be performed during a single examination.

Real-time processing of functional MR imaging data during the performance of a paradigm is available from most commercial MR imaging vendors and can be invaluable in assessing the adequacy of the paradigm being performed (36). In addition, most functional MR imaging practitioners perform detailed postprocessing (eg, motion correction, time correction, filtering, and

anatomic coregistration) to optimize the quality of the examination (35). Processing programs for this analysis are becoming more widely available, often as an integrated component of clinical scanners, workstations, and neuronavigation software packages. These processing steps can significantly alter the appearance of functional MR imaging-derived maps; a full understanding of these steps and of the limitations of functional MR imaging is mandatory for anyone performing clinical functional MR imaging examinations (35,37). Newly developed functional MR imaging techniques that do not require an active task have recently been applied clinically, and they can potentially help assess multiple cognitive domains with a single sequence (“resting state” or “functional connectivity” functional MR imaging) (38,39). These techniques are currently being evaluated and may prove useful in individuals who cannot perform active paradigms, such as young children, sedated patients, or persons with existing deficits.

Brain Mapping: Language.—Validation of functional MR imaging techniques versus other “gold standard” brain mapping techniques (usually invasive) has been performed but is limited. In the language domain, functional MR imaging has been successfully applied for purposes of documenting language laterality in both the epilepsy and brain tumor populations. Sensitivities and specificities of 90% or more have been consistently demonstrated in both populations compared with the Wada test and other invasive mapping techniques, such as electrocortical stimulation mapping (ESM) (40). Functional MR imaging is increasingly viewed as the initial test of choice for determining language lateralization in preoperative patients. However, validation of eloquent language region localization is less well defined with functional MR imaging than with invasive techniques. In a functional MR imaging–ESM study of language and motor domains in 34 consecutive patients with tumors of the eloquent brain region, Bizzi et al (41) demonstrated a language functional MR imaging sensitivity and specificity of 80% and 78%, respectively, for positive ESM sites and a 100% sensitivity in the Broca area. Higher sensitivity and specificity with lower-grade tumors may reflect the effects of cerebrovascular changes within and adjacent to higher-grade neoplasms.

Unfortunately, reported sensitivities and specificities have varied widely in previous studies, since the functional MR imaging paradigms used, methods of ESM used, and regions evaluated differ significantly among the various studies (42). In a 2013 study, Kundu et al (43) described a clear relationship between lesion-to-activation

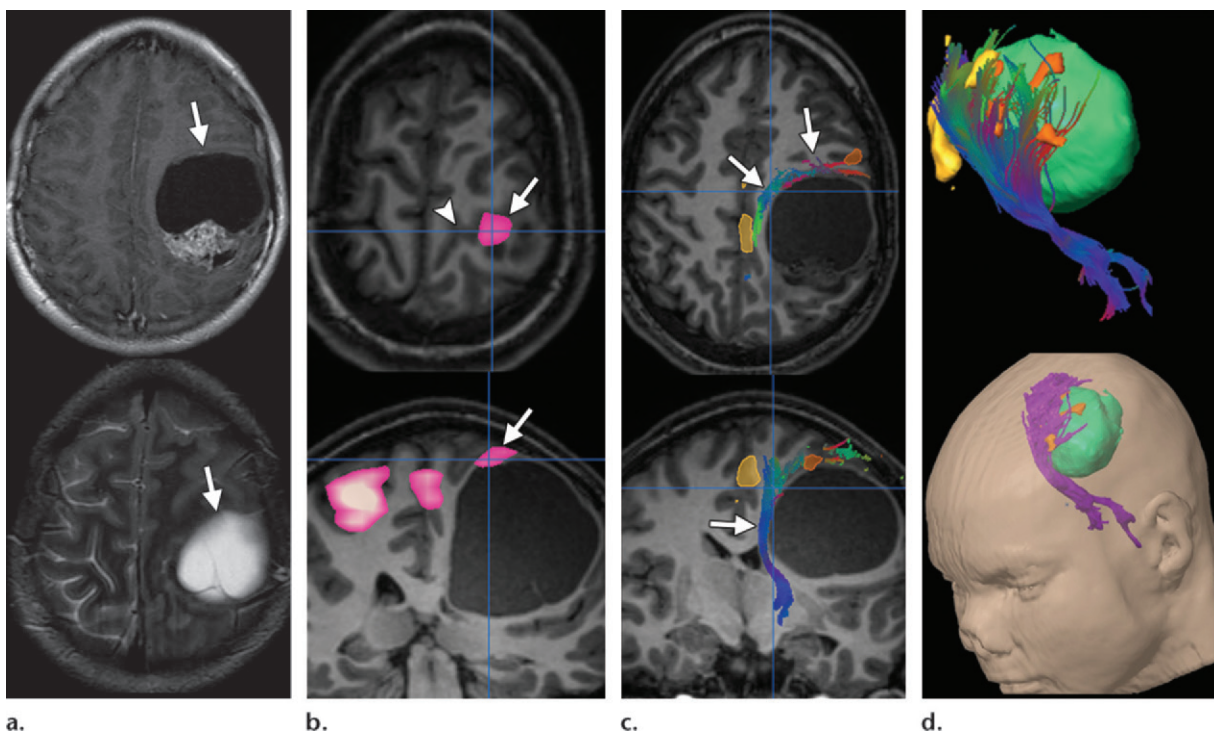


Figure 3. Anaplastic ependymoma in a 15-year-old boy with a 2-week history of progressive right hemiparesis. **(a)** Axial gadolinium-enhanced T1-weighted (top) and T2-weighted (bottom) MR images show a large left perirolandic cystic and solid tumor (arrows) obscuring typical sulcal landmarks. Definitive identification of the central sulcus was difficult. **(b)** Axial (top) and coronal (bottom) coregistered functional T1-weighted MR images obtained with a finger-tapping paradigm show a bilateral localized task-related increase in BOLD signal (activation) (pink). On the left, functional activation is displaced superiorly along the superior aspect of the mass (arrows), identifying the location of the central sulcus (arrowhead). **(c)** Functional MR imaging activation areas created with finger tapping (orange) and foot movement (yellow). Using these as regions of interest, CST tractography was performed. Note the fiber representations of the CST splayed along the anterior aspect of the mass (green) and displaced medially (arrows). **(d)** Objects created for surgical navigation (BrainLab iplan 3.0). Green = mass, purple = CST, yellow and orange = functional MR imaging activation areas. A surgical trajectory was selected that would allow access to the lesion through its posterosuperior aspect while avoiding eloquent cortex and white matter tracts. Gross total resection was performed, and no new deficits occurred thereafter.

distance in the Broca area and the extent of language lateralization with postoperative deficit in brain tumor patients. Application of multiple language paradigms to assess multiple language domains is essential for enhancing sensitivity and more fully capturing language networks preoperatively and is strongly recommended (37).

Brain Mapping: Sensorimotor Domains.—

Evaluation of sensorimotor domains has shown excellent correlation with invasive techniques and is a simple, robust method for outlining eloquent motor regions preoperatively. Reported functional MR imaging–ESM concordance rates are typically higher than with language functional MR imaging (44–47). In a study comparing the effectiveness of motor functional MR imaging and ESM in localizing the sensorimotor cortex in 26 brain tumor patients, Lehericy et al (45) demonstrated 92% accuracy for motor functional MR imaging compared with ESM. With use of 3.0-T imaging, Roessler et al (47) demonstrated 100%

agreement between functional MR imaging and ESM in 17 paracentral glioma patients.

Given the fundamental differences between functional MR imaging and invasive mapping for these domains, perfect correlation is unlikely. ESM is a disruption method that causes an arrest of function, whereas functional MR imaging is an activation-based method in which all areas are functionally active, albeit not necessarily essential, during a particular task. Nonetheless, functional MR imaging remains highly useful in decreasing surgery time for cortical and subcortical stimulation procedures and in providing a more global assessment of cerebral function in patients who cannot tolerate awake craniotomy (Figs 3, 4) (31). Additional correlation studies will likely be needed to better define clinical usefulness.

Diffusion Tensor Imaging

DTI has revolutionized the ability to evaluate white matter structures and function in both healthy and diseased states (48,49) and to define

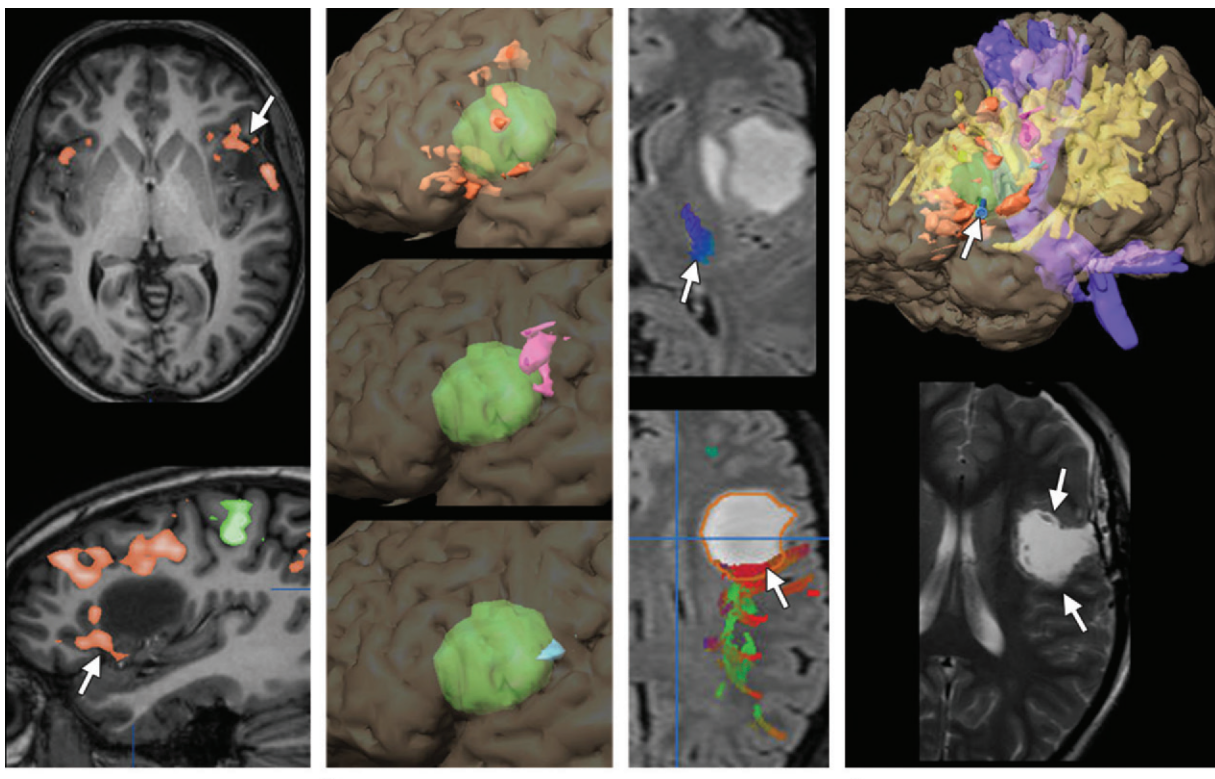


Figure 4. Grade II astrocytoma in a right-handed 17-year-old girl with headache. The patient proved to have a non-enhancing mass in the left inferior frontal lobe but could not tolerate awake craniotomy. **(a)** Covert verb generation functional MR images demonstrate areas of activation along the periphery of the tumor, especially laterally and anteriorly, with orange indicating covert verb generation and green indicating finger tapping. Arrows = activation in the left inferior frontal gyrus (pars opercularis and triangularis). **(b)** Three-dimensional objects created from three functional MR imaging paradigms performed to more comprehensively evaluate areas related to speech production. The tumor is shown in green, with orange indicating covert verb generation, pink indicating tongue movement, and blue indicating phonation. **(c)** DTI-based tractography of the CST (top) and arcuate fasciculus (AF)—superior longitudinal fasciculus (bottom) demonstrate fiber representations close to (CST) and in direct contact with (AF) the tumor (arrows). **(d)** Combined functional MR-diffusion tensor image (BrainLab iplan 3.0) (top) shows the planned surgical trajectory (arrow). Intraoperative MR image (bottom) obtained after gross total resection shows the surgical cavity (arrows). No postoperative language deficits were noted.

the anatomy of eloquent white matter tracts for surgical planning (49,50). Standard DTI models the morphology, magnitude, and direction of brain water movement as a tensor quantity on a voxel-by-voxel basis (48). Multiple techniques essentially connect voxels with similar water diffusion characteristics between areas of functional and anatomic interest (with certain user-defined restrictions); these connections allow the development of diffusion-related “tracts” to be resolved reflecting major white matter bundles (49,50). Numerous deterministic regions of interest and probabilistic (global) approaches to tractography have been suggested and applied (51). Various software and processing solutions for providing clinically useful “fiber streamline” representations are available from clinical MR and neuronavigation software vendors. As with functional MR imaging processing, a thorough understanding of the processing techniques and

limitations of DTI-based tractography is mandatory for performing clinical DTI-derived tractography examinations.

Validation of standard DTI-based tractography has been performed primarily by correlating findings with the results of subcortical stimulation mapping. In the CST, results have been encouraging, with positive stimulation to CST tractography distances usually identified within 10 mm (52–54). In a large, randomized prospective study of 238 patients, Wu et al (55) demonstrated the clear benefit of incorporating CST tractography during neuronavigation for tumor surgery; specifically, patients who underwent CST tractography had greater resection, better postoperative neurologic function, and longer survival than did those who did not. In the AF, correlations are less well defined. Kamada et al (56) demonstrated good correlation between combined functional MR imaging—tractography of the AF

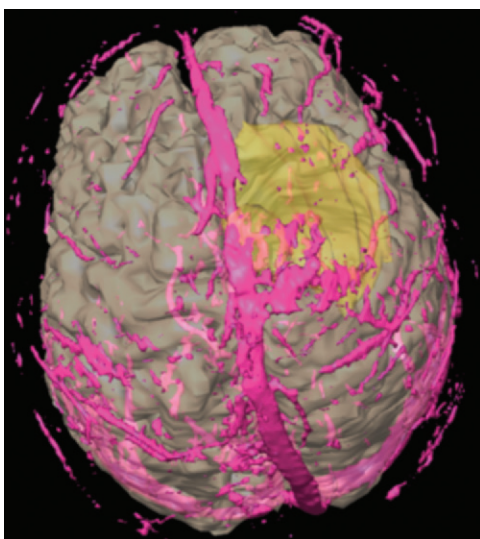


Figure 5. Three-dimensional image of a large parasagittal meningioma with integrated MR venographic data (pink) shows the superior sagittal sinus and important draining cortical veins on the posterior aspect of the tumor (yellow) that will need to be preserved at surgery.

and subcortical stimulation in two patients with frontotemporal brain tumors. Leclercq et al (57) described an 81% concordance rate between subcortical stimulation and the DTI-derived AF in 10 patients with language region neoplasms. Figure 3 demonstrates visualization of the AF and CST for surgical guidance.

Two major drawbacks of standard DTI are its inability to resolve regions of “crossing fibers” and difficulty in determining fiber terminations (58). These limitations can lead to incomplete and inaccurate results in defining important white matter tracts. Newer techniques for water diffusion detection and data processing that can rectify some of these limitations include high-angular resolution diffusion imaging (58,59) and high-definition fiber tracking (60). Although initial clinical results for these techniques are promising, their application is not yet widespread.

Teaching Point

Functional MR imaging and DTI-based tractography have become useful tools in preoperative assessment and imaging-guided surgical therapy in patients with brain tumors in or near eloquent brain regions. Despite having limitations, the incorporation of functional MR imaging and DTI into surgical planning (functional neuronavigation) can alter the surgical approach, allow greater resection, and limit postoperative deficits in these patients (31). The use of functional MR imaging and DTI does not preclude standard intraoperative assessments of eloquent cortex and white matter tracts. In fact, an approach in which the neurosurgeon

combines functional MR imaging–DTI with intraoperative functional assessments may lead to optimal outcomes (31).

Imaging in Neurosurgery

Surgical Integration

Brain tumor surgery has come a long way since the days of Harvey Cushing, who operated using only x-rays and pneumoencephalograms to localize tumors with no more than a light bulb taped to his forehead for illumination. Many advances in modern neurosurgery, especially with respect to brain tumors, are directly and intimately interwoven with advances in neuroimaging. Neurosurgeons now routinely use multiple advanced imaging modalities for brain tumor surgery, including MR angiography and MR venography to evaluate vascular structures and functional MR imaging and DTI to localize functional areas (Fig 4) (61). With imaging-guided surgery, these modalities are introduced directly into the operating room to help localize tumors and guide tumor resection.

Vascular Imaging

Brain surgeons acknowledge the importance of imaging, not only for accurately identifying the arteries and veins that supply a tumor, but also for visualizing vessels that must be preserved to maintain patient function. Angiography remains effective as a preoperative tool for identifying tumor feeding vessels and allowing embolization, especially in vascular tumors (eg, meningiomas). Using computer-generated image-guided systems, neurosurgeons can now integrate CT and MR angiographic-venographic data with conventional imaging data, applying these data in the operating room to help guide the surgical approach and preserve important arteries and veins (Fig 5).

Functional MR

Imaging–DTI and Neurosurgery

Before the development of functional MR imaging and DTI, the only way to localize functional areas of the brain and important white matter structures such as the CST was with use of direct intraoperative electrophysiologic mapping. This was laborious for both the surgeon and the patient, adding time to surgery and increasing risks (eg, intraoperative seizures). However, functional MR imaging and DTI allow preoperative localization of functional areas that can be integrated into intraoperative guidance systems (Figs 3, 4) (62). We have found the use of functional MR imaging–DTI with imaging-guided surgery in the operating room to be highly sensitive in predicting whether surgery in or near an eloquent brain



Figure 6. Photograph illustrates imaging-guided surgery, with active localization of a tumor using a pointer and images displayed on a computer screen.

region would lead to a deficit for that patient. When functional MR imaging showed tumors near but not invading an eloquent region and surgery did not violate these functional areas, patients did not develop long-term neurologic deficits from surgery (63).

Imaging-guided Surgery

Advanced neuroimaging techniques are valuable to the neurosurgeon, especially when brought into the operating room for real-time use. Computer-based neuronavigation consists of a tracking system that fuses with conventional and advanced imaging. A camera “displays” the patient so that the surgeon can track the tumor and the patient’s position on a computer screen using a live pointer (Fig 6) (see <http://youtu.be/tJTR4ty0BW4>).

Integration with modern neuroimaging tools such as MR angiography, MR venography, functional MR imaging, and DTI allows application of these data in the operating room. However, such information must still be obtained prior to surgery. The addition of intraoperative MR imaging takes advanced real-time imaging to the next level; for example, the surgeon can see whether maximal resection of a tumor has been achieved while accounting for brain shift changes related to surgery. Multiple studies and one randomized trial have demonstrated that the use of intraoperative MR imaging significantly improves the extent of resection, especially for gliomas and pituitary adenomas (64–66).

In summary, neurosurgery as a whole, and brain tumor surgery in particular, have benefited greatly from advances in neuroimaging that include MR imaging, MR angiography, MR venography, functional MR imaging, and DTI. These techniques are used daily by brain surgeons to help achieve the best possible resection with the fewest side effects for patients. Intraoperative MR imaging is developing into a key tool for brain tumor surgery, and future advances in neurosur-

gery will undoubtedly be directly tied to advances in neuroimaging.

Imaging in Radiation Therapy

Imaging is essential for the planning and delivery of radiation therapy in patients with brain tumors. From the patient’s initial evaluation and staging, to the definition of the radiation therapy targets, to the daily verification of radiation beam placement and evaluation of the treatment effects, imaging plays an indispensable role.

Simulation

Virtually all radiation therapy for CNS tumors begins with a planning visit known as “simulation.” A rigid immobilization mask is constructed that will position and keep the patient’s head still during each daily treatment session. Next, a CT scan of the patient’s head is performed while the mask is in place. This so-called anchor scan defines the spatial orientation of the patient’s head relative to the treatment beams and the electron density of the tissues that are used for calculating radiation distribution (isodoses) during the treatment-planning process. With use of this CT anchor scan, additional images, including conventional MR, positron emission tomographic (PET), and functional MR images, are fused into a composite image that will help define the radiation therapy targets.

During radiation treatment planning, these fused images may be used to define (*a*) visible tumor, (*b*) pathways of potential tumor spread, (*c*) critical normal structures to be protected from radiation, and (*d*) biologic differences within a tumor that may be exploited with use of differing radiotherapeutic strategies.

Imaging to Define Visible Tumor

A postoperative MR image obtained in a patient with GBM can be fused with the patient’s treatment-planning CT scan (Fig 7). Tumor is identified on the basis of enhancement on T1-weighted

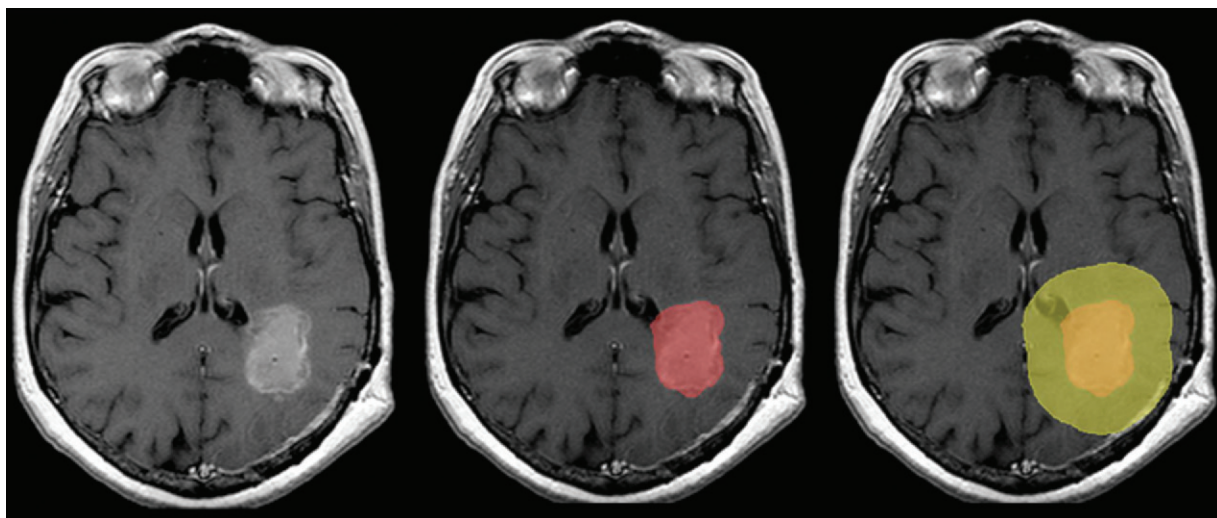


Figure 7. Fusion of a postoperative MR image (left) obtained in a patient with GBM with the patient's treatment-planning CT images (middle and right). Pink = gross tumor volume (GTV); yellow = clinical target volume (CTV), which indicates possible microscopic spread.

MR images. In addition, areas of surrounding edema often contain tumor cells (67) and are sometimes included in the primary radiation therapy target, also known as the gross tumor volume or GTV; this volume is usually best defined with a T2-weighted FLAIR imaging protocol. Imaging technique can affect the appearance and therefore the volume of target tissue; for example, volumes on FLAIR images may differ depending on the inversion time and repetition time, as well as scanner strength (68). Collaboration between a diagnostic radiologist and a radiation oncologist is helpful in choosing the imaging study and technique that are most appropriate for identifying the volume of interest.

Other imaging modalities can be effective in defining the tumor volume for radiation therapy. For example, in a case involving a meningioma with both a dural and intradiploic component, the patient underwent near-total resection, with lingering suspicion for a small amount of residual tumor (Fig 8). Pathologic analysis showed a grade II meningioma, and postoperative radiation therapy was recommended to prevent recurrence. No residual tumor was seen on postoperative CT or MR images, and a ¹¹C methionine PET scan was performed, which demonstrated a small area of residual tumor within the larger surgical bed. Subsequently, the radiation therapy treatment volume was significantly reduced, with an accompanying decrease in treatment morbidity.

Imaging to Define Pathways of Tumor Spread

Radiation therapy is often used to prophylactically treat the pathways of spread in tumors that spread microscopically beyond the radiologically

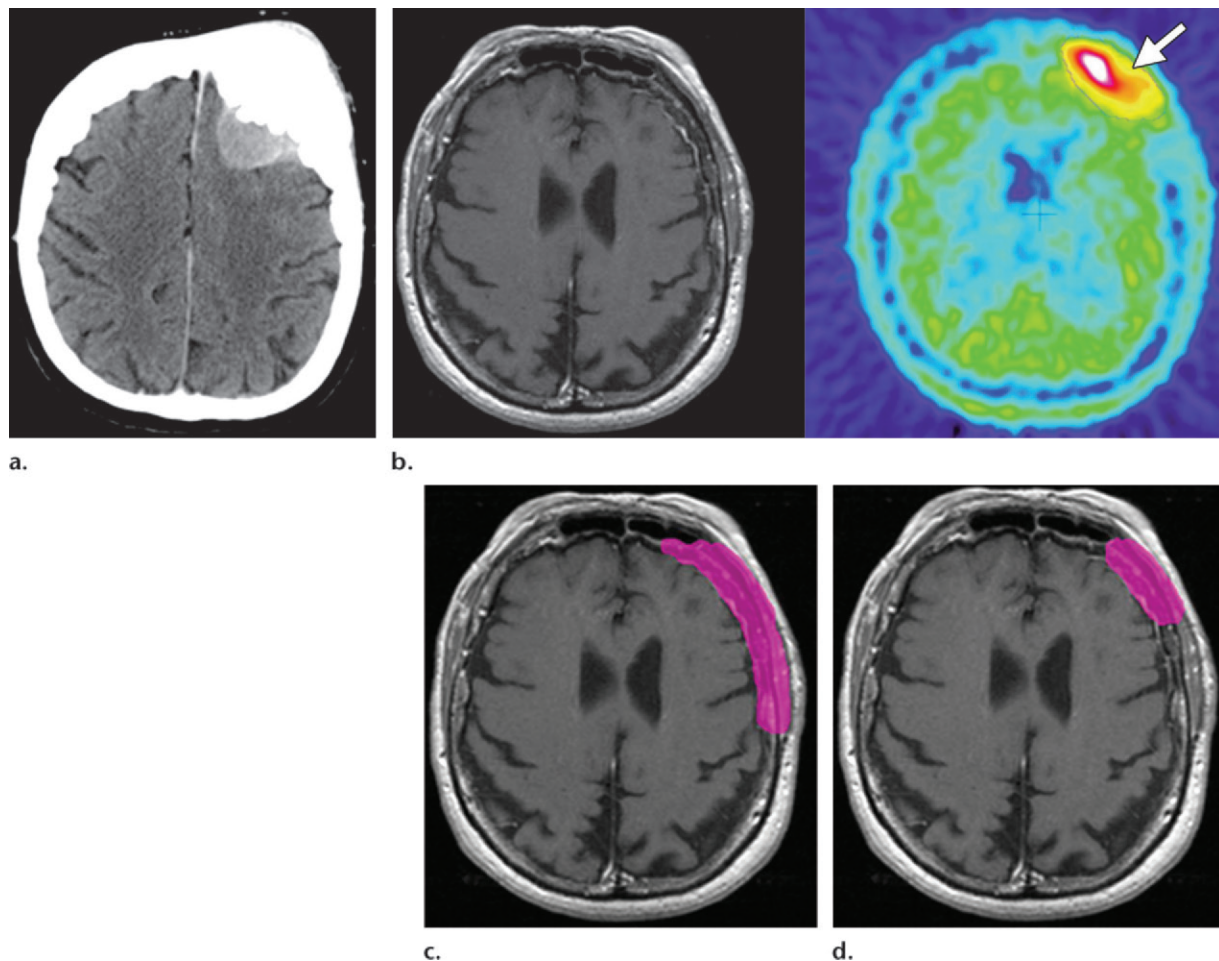
identifiable target volume. This part of the radiation therapy target volume is called the clinical tumor volume or CTV. In the treatment of glioblastoma, the CTV is often simply defined as a geometric enlargement of the GTV by 1–2 cm. However, because glioblastoma preferentially spreads along white matter tracts, recent work has investigated the use of tractography to construct a more “intelligent” CTV (69). Further study is needed, but these imaging techniques may in the future become a valuable part of radiation therapy planning for gliomas.

Imaging to Define Normal Tissue

Imaging is also used to identify normal anatomy that is to be avoided during radiation therapy. For example, in a case of recurrent GBM in a patient who had undergone radiation therapy and chemotherapy, stereotactic radiosurgery was recommended to treat the area of recurrence (Fig 9). With the fusion of functional MR imaging and radiation treatment-planning imaging, the multidisciplinary team was able to devise a radiation treatment to minimize additional exposure to this eloquent brain region.

In another case involving an 8-year-old boy with medulloblastoma, the intraoperative imaging findings and the surgeon’s inspection of the surgical site showed complete resection. However, postoperative MR imaging showed an enhancing lesion in the left cerebellar hemisphere that was suspicious for residual tumor. Characterization of this imaging abnormality was critical: The patient would either face an aggressive, morbid regimen of radiation therapy and chemotherapy for residual tumor, or he would avoid this regimen if the abnormality represented postoperative changes.

Figure 8. Residual tumor after near-total resection in a patient with meningioma. **(a)** Preoperative CT image shows a prominent intradiploic tumor. **(b)** Postoperative MR image (left) shows no residual tumor, whereas a carbon 11 (¹¹C) methionine PET image (right) shows residual intradiploic meningioma (arrow). **(c)** Radiation therapy target volume (pink) superimposed on the MR image in **b** shows the volume that would require treatment based only on the preoperative MR imaging–CT location of the tumor. **(d)** Radiation therapy target volume (pink) superimposed on the MR image in **b** shows the volume that was treated based on the ¹¹C methionine PET image.



Multivoxel spectroscopy supported the clinical impression of complete resection (Fig 10), allowing the patient to be treated with a less aggressive regimen.

Imaging to Define Tumor Biology for “Personalized” Radiation Therapy

A number of biologic factors affect tumor response to radiation therapy, some of which can be assessed with imaging. Because hypoxia of tumor tissue is associated with resistance to radiation therapy, a higher radiation dose is required. PET can help detect hypoxic areas in a portion of the tumor, which can then be targeted to receive a higher radiation dose (70).

CT and MR imaging are an indispensable part of radiation therapy planning. Ultimately, outcomes from radiation therapy are only as good as the imaging on which they are based. Newer modalities, such as functional and metabolic im-

aging, are now being incorporated into the planning process and have the potential to decrease treatment-related morbidity and improve tumor control.

Posttreatment Imaging

Assessment of therapy often starts with an initial postoperative scan to determine the required degree of surgical resection. If clinically feasible, postoperative imaging should be performed within the first 24 hours. Although mild reactive enhancement can be present immediately after surgery, nodular or masslike enhancement seen within 24 hours typically represents residual tumor (Fig 11) (71). Distinguishing enhancing tumor from reactive change on delayed images can be difficult. Also, early postoperative T2-weighted FLAIR imaging may be helpful in differentiating between areas of residual nonenhancing tumor and postsurgical reaction.

Teaching Point

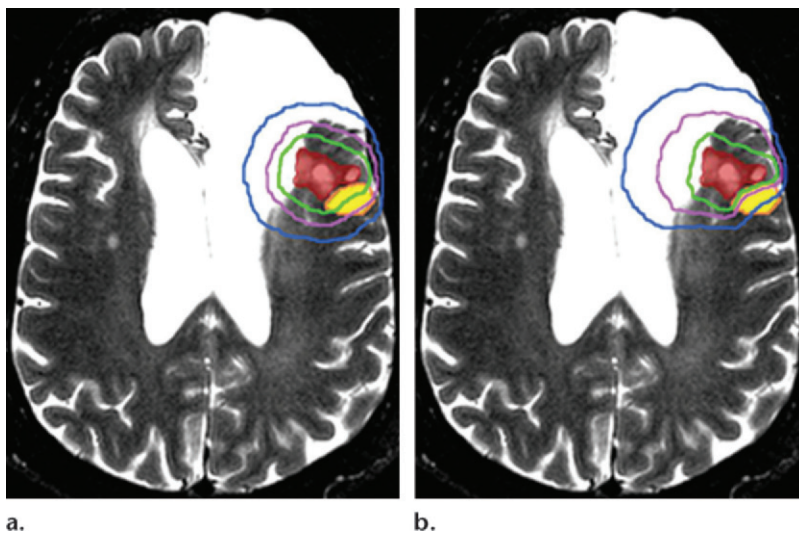
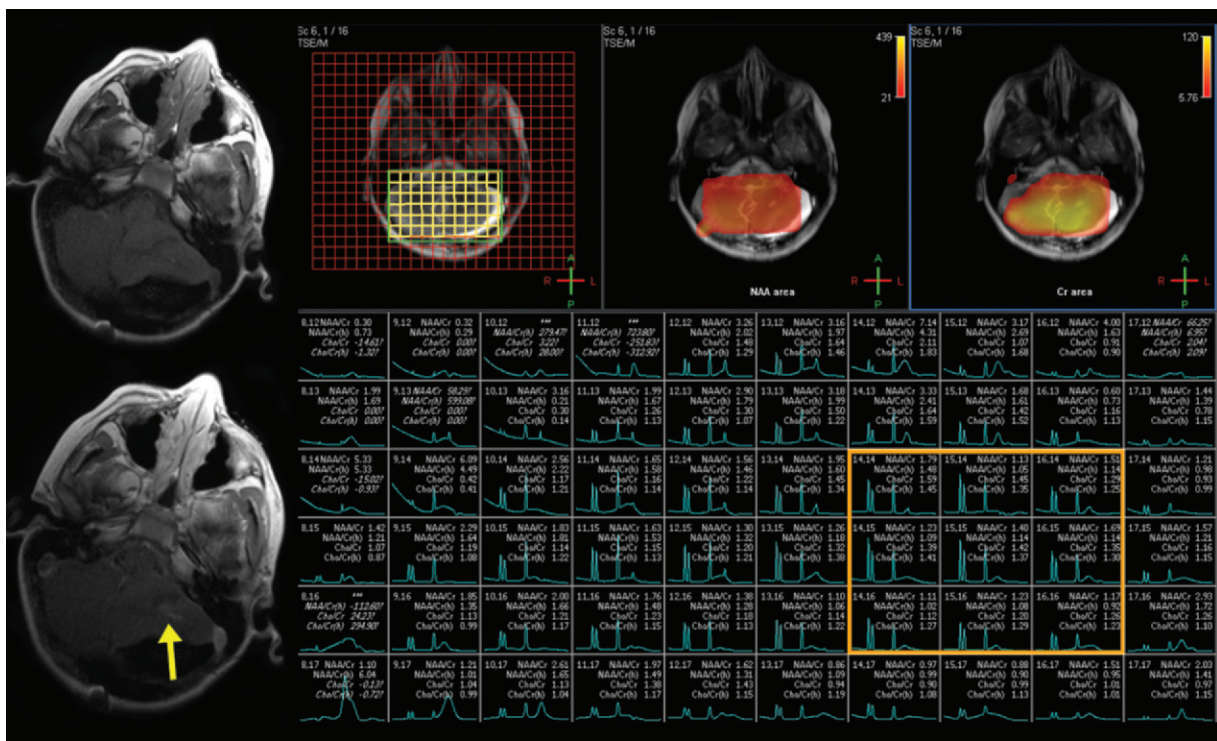


Figure 9. Recurrent GBM in a patient who had previously undergone radiation therapy and chemotherapy. Functional MR images show radiation treatment isodoses that were planned prior to (a) and after (b) obtaining the image, with sparing of the Broca area (yellow) from high-dose radiation. Red = recurrent tumor.

Figure 10. Postoperative change in an 8-year-old boy with medulloblastoma. Preoperative MR spectroscopy demonstrated aggressive features. Intraoperative precontrast (top left) and postcontrast (bottom left) T1-weighted MR images show an area of concern for residual tumor (arrow). Multivoxel spectroscopic images (top middle and right) (box at bottom right indicates data representing the region of enhancement) show mildly decreased NAA and a mildly elevated choline level, neither of which findings is characteristic of aggressive tumor behavior. The findings support a diagnosis of postoperative change rather than residual tumor.



In addition, postoperative hemorrhage may demonstrate T1 shortening and may be difficult to distinguish from an enhancing lesion. Therefore, direct comparison of pre- and postcontrast images, preferably obtained in the same imaging plane, is important (Fig 12).

Changes in the signal intensity of fluid within the resection cavity of partially resected gliomas can be very helpful in assessing posttreatment im-

ages. Winterstein et al (72) demonstrated that the development of increased signal intensity within the postoperative cavity on FLAIR images is very specific for tumor progression and may be seen prior to an increase in tumor size.

DW Imaging

DW imaging is becoming increasingly important in the assessment of treatment results in patients

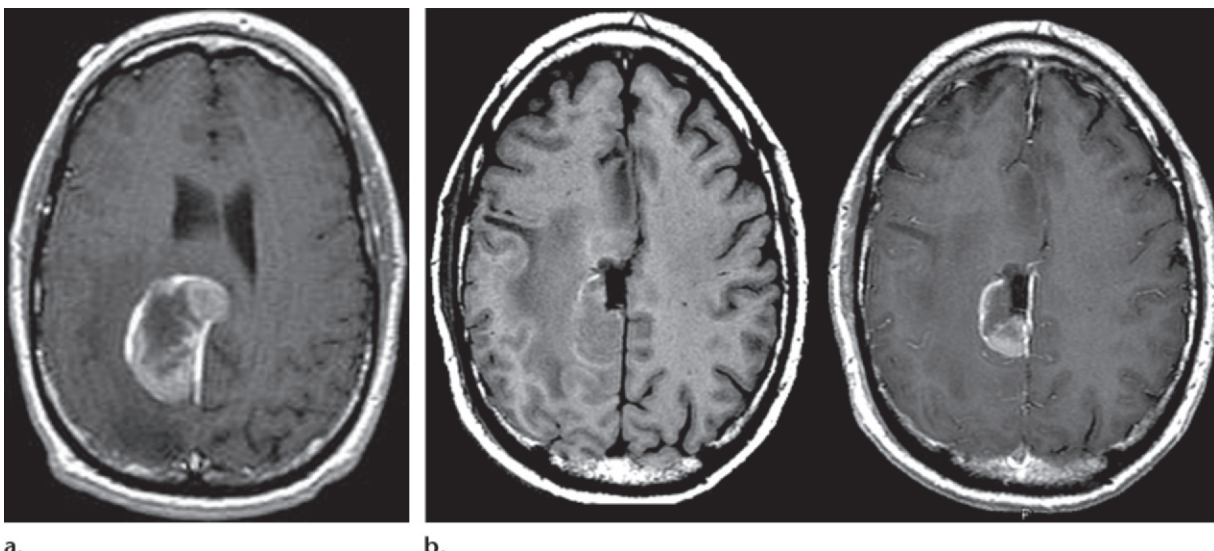


Figure 11. Residual right parasagittal parietal GBM. **(a)** Preoperative gadolinium-enhanced T1-weighted image shows an enhancing mass in the right parasagittal parietal lobe. **(b)** Axial precontrast (left) and gadolinium-enhanced (right) T1-weighted images obtained within 24 hours of surgery. The precontrast image shows a small amount of T1 hyperintensity consistent with blood products. The postcontrast image shows a nodular area of enhancement along the posterior aspect of the surgical cavity, a finding that is suspicious for residual tumor (confirmed at repeat surgery).

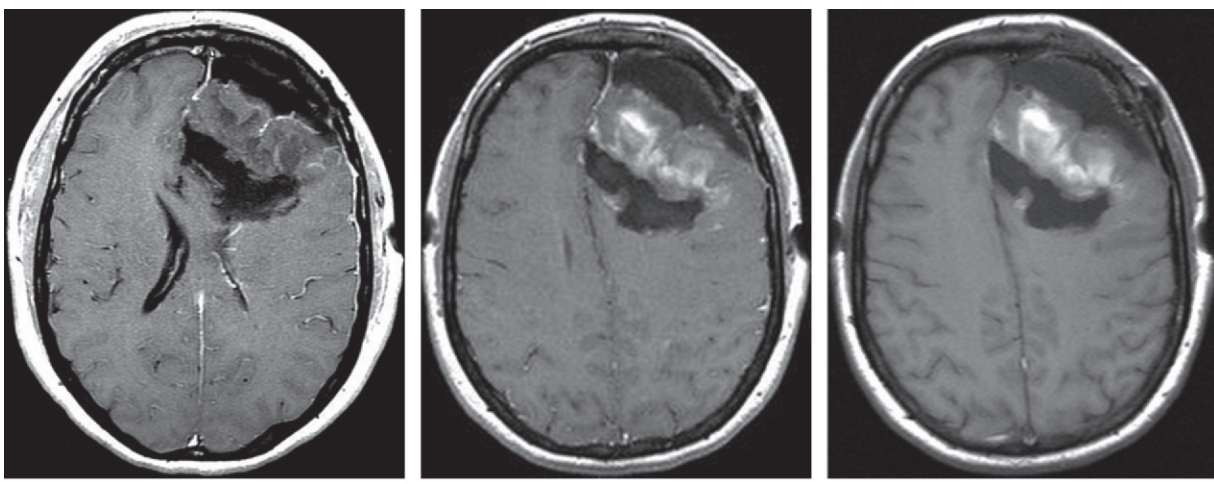


Figure 12. Postsurgical subacute hemorrhage in a 56-year-old patient with left frontal GBM. **(a)** Postoperative T1-weighted image obtained within 24 hours of surgery shows no evidence of a residual enhancing mass. **(b)** Contrast-enhanced radiation treatment-planning MR image obtained 3 weeks after surgery shows an area of T1 hyperintensity that was misinterpreted as enhancement representing early tumor recurrence because no precontrast T1-weighted sequence had been performed; hence, the prognosis was deemed very poor. **(c)** Follow-up precontrast T1-weighted image obtained a few days later shows evolving subacute hemorrhage in the surgical bed that corresponds to the T1-hyperintense signal seen in **b**. The image shows no significant enhancement compared with the nonenhanced image and, therefore, no recurrent enhancing tumor.

with brain tumors. On images obtained immediately after surgery, areas of restricted diffusion resulting from surgical resection or ischemia may be seen around the surgical cavity. At follow-up imaging, these areas may demonstrate enhancement that mimics tumor recurrence. Therefore, comparison of new areas of enhancement with areas of restricted diffusion seen at immediate

postoperative imaging is important (Fig 13). If these areas match, the enhancement most likely represents reactive changes or subacute enhancing ischemia rather than recurrent tumor.

DW imaging can also be helpful in detecting early tumor recurrence, especially in nonenhancing lesions (73,74). If a new or enlarged area of signal abnormality and restricted diffusion is seen

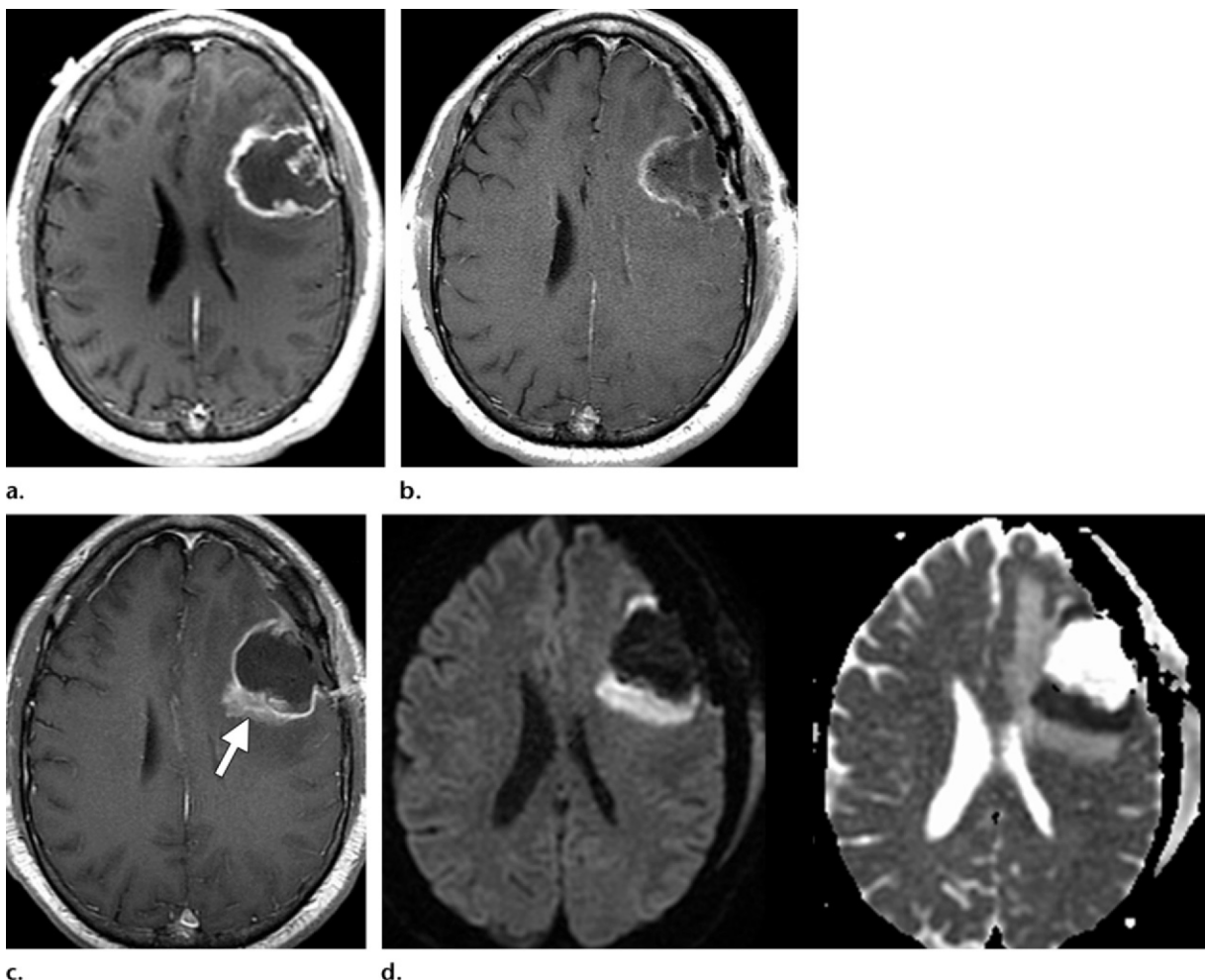


Figure 13. Postsurgical change in a patient with left frontal GBM. **(a)** Axial gadolinium-enhanced T1-weighted image from a preoperative planning study demonstrates a ring-enhancing, centrally necrotic mass in the left frontal lobe. **(b)** Gadolinium-enhanced T1-weighted image obtained 12 hours after surgery demonstrates thin, curvilinear T1 shortening at the surgical margin, a finding that represents primarily hemorrhage. **(c)** Gadolinium-enhanced T1-weighted image obtained at a different institution 3 weeks after surgery demonstrates irregular nodular enhancement (arrow) along the posterior margin of the surgical cavity. (Precontrast T1-weighted imaging had shown no hemorrhage.) This enhancement was interpreted as recurrent tumor, and the patient was denied entrance into a clinical trial. **(d)** Viewed retrospectively, DW (left) and ADC (right) images from the study performed 12 hours after surgery demonstrate diffusion restriction along the posterior margin of the cavity, a finding that corresponds to the new area of enhancement. Therefore, the enhancement represents postsurgical change and reaction rather than recurrent tumor.

in a postoperative margin that previously had demonstrated no restricted diffusion, tumor recurrence is likely (Fig 14) (75).

Bevacizumab (Avastin; Genentech, South San Francisco, Calif) is a commonly used antiangiogenic agent that can result in interesting and sometimes confusing posttreatment imaging findings. Bevacizumab is a recombinant monoclonal immunoglobulin G antibody that binds to vascular endothelial growth factor. A rapid, marked decrease in, or even resolution of, enhancement can be observed because of decreased neovascularity and near normalization of tumor vessels. However, this finding should be interpreted cautiously and in conjunction with findings at T2-weighted FLAIR imaging.

Tumor recurrence often manifests as recurrent or new abnormal T2 prolongation without enhancement (76,77). The presence of associated restricted diffusion further supports a finding of recurrent tumor (Fig 15).

Radiation Necrosis versus Recurrence

As a potential long-term complication of radiation therapy and chemotherapy, radiation necrosis can occur months to decades after treatment. It is related to the total radiation dose and fraction size, as well as lesion location and size, patient age, and vascular risks. Histologic findings are characterized by endothelial damage and vascular hyalinization, leading to occlusive vasculopathy and ischemic changes. Radiation

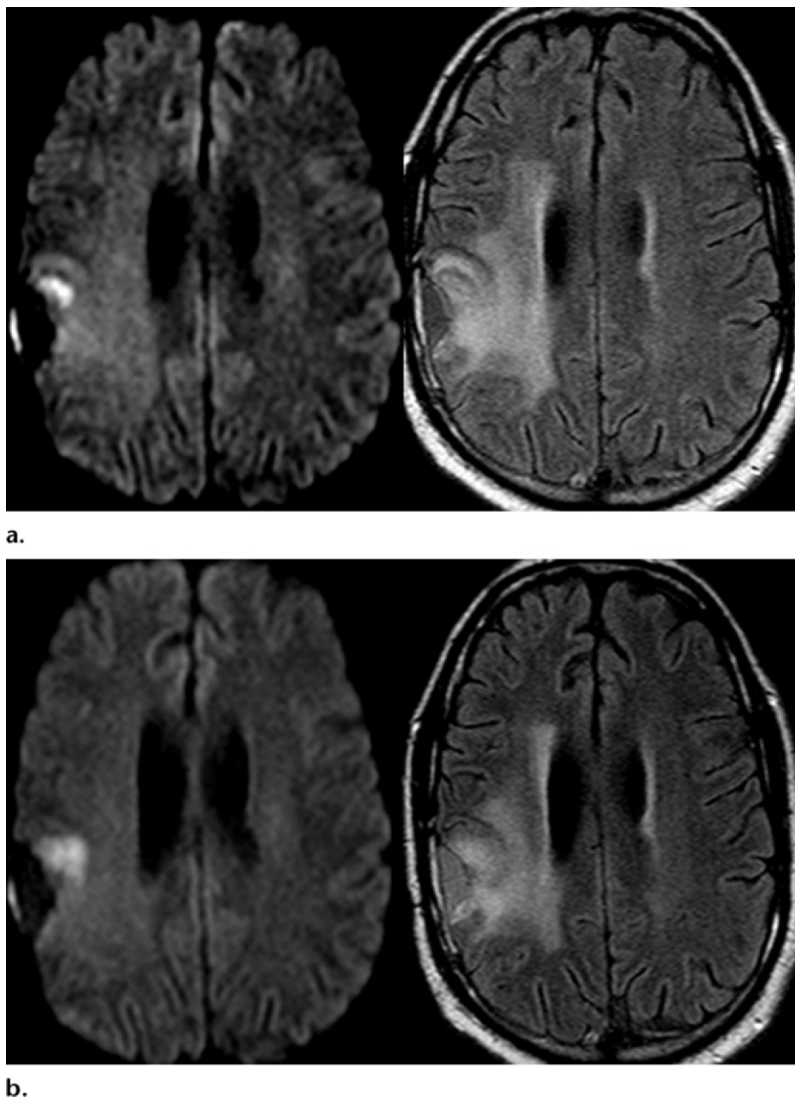


Figure 14. Recurrent tumor in a patient with right parietal GBM who was treated with surgery, radiation, and temozolomide. (a) DW (left) and T2-weighted FLAIR (right) images obtained 1 year after treatment demonstrate a small area of new diffusion restriction adjacent to the surgical cavity, with associated hyperintense signal on the FLAIR image. (b) DW (left) and T2-weighted FLAIR (right) images obtained 3 months later demonstrate increased diffusion restriction. At 6-week follow-up, the patient had new enhancement and clear evidence of tumor recurrence.

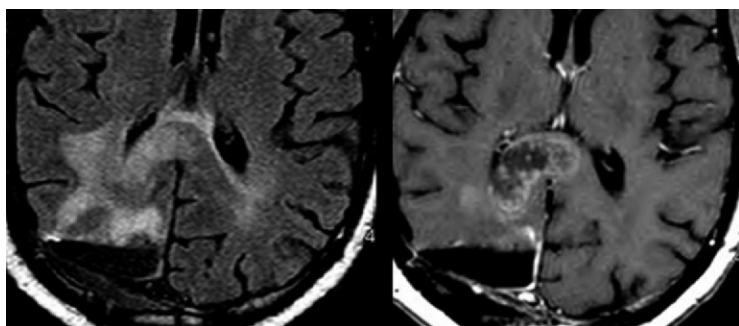
necrosis usually occurs near the site of the original tumor and within the margins of the irradiation field (78).

Radiation necrosis is characterized by areas of enhancement, T2 prolongation, and significant edema that can mimic tumor recurrence on conventional images. The degree of edema and mass effect is often disproportionate to the size of the enhancing lesion. Both MR spectroscopy and perfusion MR imaging are useful in increasing diagnostic confidence (79,80). Recurrent high-grade gliomas and metastases typically demonstrate significantly elevated relative CBV ratios (Fig 16), whereas radiation necrosis is associated with a reduction in relative CBV or hypoperfusion (80,81). MR spectroscopy of radiation necrosis is characterized by large lactate-lipid doublets with relative reduction of other metabolites (26). In many cases, the findings at MR spectroscopy and perfusion MR imaging will be relatively specific; however, there is often concomitant tumor and radiation necrosis that can produce

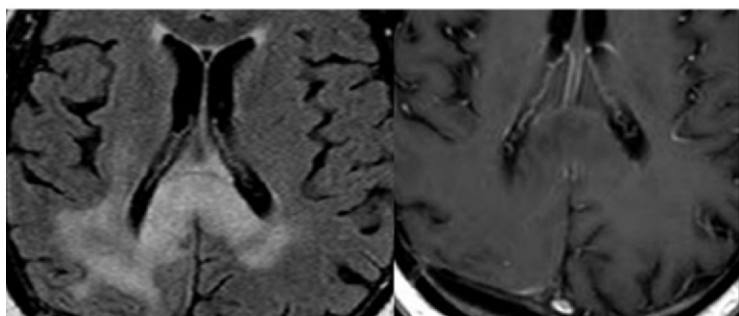
nonspecific or confusing results (82). Follow-up imaging is crucial in these circumstances.

Pseudoprogression

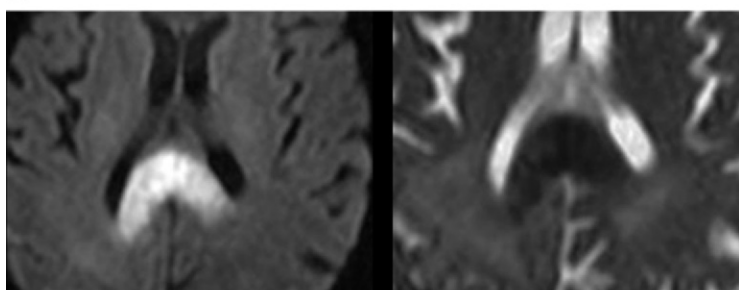
In 20%–40% of patients with CNS neoplasms who undergo radiation therapy and adjuvant chemotherapy, both the size and the associated T2 prolongation of the enhancing lesion temporarily increase, a phenomenon known as pseudoprogression (Fig 17) (83–85). These findings can simulate tumor progression and treatment failure, possibly resulting in the inappropriate discontinuation of effective therapy. Pseudoprogression occurs more often in patients who undergo concurrent radiation therapy and chemotherapy, typically within 6–12 weeks after treatment. Pseudoprogression is histologically similar to radiation necrosis, with enlarging areas of enhancement that are thought to represent local inflammatory response and increased vascular permeability. Patients are often clinically asymptomatic, and studies suggest an association with increased survival (86).



a.



b.



c.

Figure 15. Recurrent tumor in a 45-year-old man with GBM. **(a)** Routine follow-up T2-weighted FLAIR (left) and gadolinium-enhanced (right) images demonstrate new enhancement in the splenium. **(b)** Gadolinium-enhanced images obtained after six infusions of bevacizumab show an increase in nonenhancing abnormal T2 prolongation in the splenium, despite complete resolution of the enhancing lesion. **(c)** DW (left) and ADC (right) images demonstrate restricted diffusion with reduced ADC values in the area of increased FLAIR signal (cf **a**), findings that are suggestive of tumor. The discordance between progressive nonenhancing tumor and decreased enhancement is a recognized effect of antiangiogenic agents. Findings at metabolic imaging supported the diagnosis of recurrent tumor.

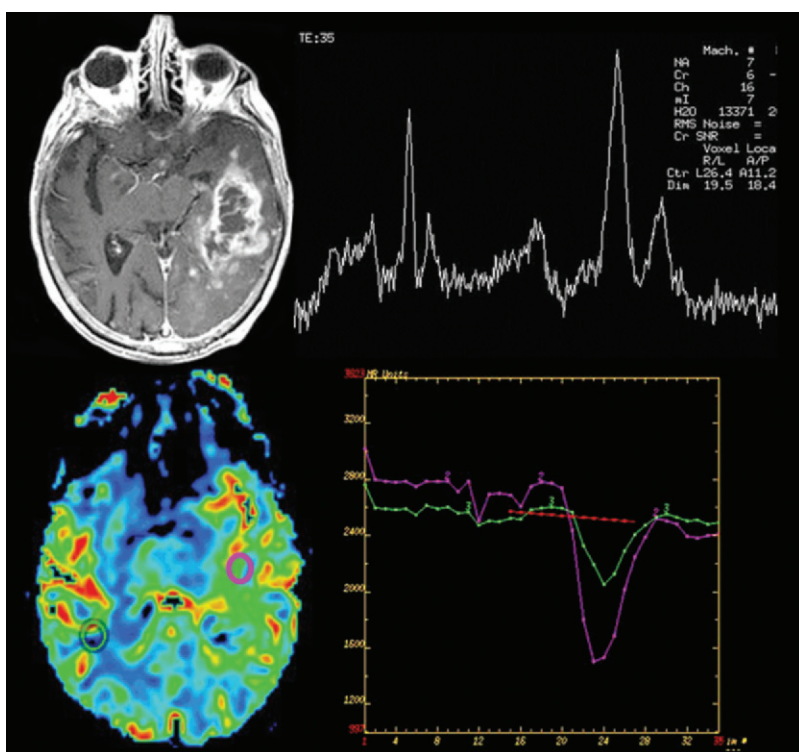
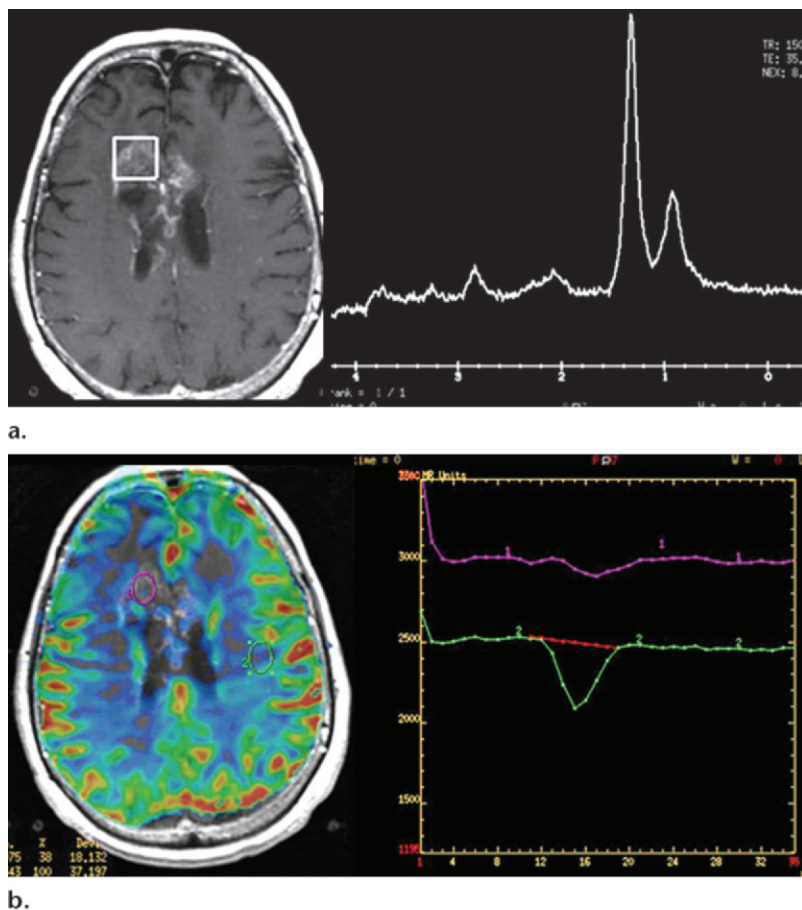


Figure 16. Recurrent high-grade tumor in a patient with GBM who had undergone radiation therapy and chemotherapy. Follow-up post-contrast T1-weighted image (top left) shows progressive irregular nodular enhancement in the left temporal lobe, corresponding to the area of previous tumor resection and treatment. MR spectroscopic image (TE = 35 msec) (top right) obtained in the area of enhancement demonstrates a large lactate-lipid doublet; however, other metabolites are also present, with marked elevation of the choline-creatinine ratio. DSC perfusion MR image (bottom left) demonstrates green within the region of interest (hot pink circle) overlying the enhancing lesion, compared to blue in the contralateral white matter. Time-signal intensity graph (bottom right) shows a relative CBV ratio of 2.13, consistent with hyperperfusion. These findings represent recurrent high-grade tumor.

Figure 17. Pseudoprogression in a 50-year-old man with frontal GBM who had undergone treatment with a combination of radiation and temozolomide. **(a)** Follow-up MR image (left) obtained 4 weeks after treatment shows a progressive area of enhancement (box) in the right frontal region. Clinically, the patient was doing well. MR spectroscopic image (TE = 35 msec) (right) obtained in the area of enhancement demonstrates a large lipid-lactate peak and relative lack of choline elevation. **(b)** DSC perfusion image (left) demonstrates no change in the color mapping of the enhancing lesion compared to the contralateral white matter. Time-signal intensity graph (right) shows a relative CBV ratio of 0.38 consistent with hypoperfusion. The patient's clinical presentation, combined with the timing of the imaging changes and MR spectroscopy-perfusion findings, are consistent with pseudoprogression. On subsequent images, the area of enhancement was reduced in size.



Pseudoprogression may demonstrate findings at MR spectroscopy and perfusion MR imaging that are similar to those of radiation necrosis, including a decrease in the relative CBV ratios within the enhancing lesion (87). However, the findings are often nonspecific. Therefore, recognition of this phenomenon, correlation with the type and timing of treatment, and sometimes additional imaging with PET (88) are important.

Conclusion

Imaging plays a vital role in the diagnosis and treatment of patients with brain tumors. Conventional CT and MR imaging as well as more advanced imaging techniques are increasingly being used by referring neurosurgeons, radiation oncologists, and neuro-oncologists to help guide patient management. As quickly as new imaging techniques develop, our nonradiologist colleagues adopt them into their practices, underscoring the central role that radiology plays on the multidisciplinary brain tumor team.

References

- Law M. Advanced imaging techniques in brain tumors. *Cancer Imaging* 2009;9(Spec No A):S4–S9.
- Jenkinson MD, Du Plessis DG, Walker C, Smith TS. Advanced MRI in the management of adult gliomas. *Br J Neurosurg* 2007;21(6):550–561.
- Yang E, Nucifora PG, Melhem ER. Diffusion MR imaging: basic principles. *Neuroimaging Clin N Am* 2011;21(1):1–25, vii.
- Yamasaki F, Kurisu K, Satoh K, et al. Apparent diffusion coefficient of human brain tumors at MR imaging. *Radiology* 2005;235(3):985–991.
- Kanekar SG, Zacharia T, Roller R. Imaging of stroke. II. Pathophysiology at the molecular and cellular levels and corresponding imaging changes. *AJR Am J Roentgenol* 2012;198(1):63–74.
- Schwartz KM, Erickson BJ, Lucchinetti C. Pattern of T2 hypointensity associated with ring-enhancing brain lesions can help to differentiate pathology. *Neuroradiology* 2006;48(3):143–149.
- Hygino da Cruz LC Jr, Vieira IG, Domingues RC. Diffusion MR imaging: an important tool in the assessment of brain tumors. *Neuroimaging Clin N Am* 2011;21(1):27–49, vii.
- Sutherland T, Yap K, Liew E, Tartaglia C, Pang M, Trost N. Primary central nervous system lymphoma in immunocompetent patients: a retrospective review of MRI features. *J Med Imaging Radiat Oncol* 2012;56(3):295–301.
- Zacharia TT, Law M, Naidich TP, Leeds NE. Central nervous system lymphoma characterization by diffusion-weighted imaging and MR spectroscopy. *J Neuroimaging* 2008;18(4):411–417.
- Hakyemez B, Erdogan C, Yildirim N, Parlak M. Glioblastoma multiforme with atypical diffusion-weighted MR findings. *Br J Radiol* 2005;78(935):989–992.

11. Stadnik TW, Chaskis C, Michotte A, et al. Diffusion-weighted MR imaging of intracerebral masses: comparison with conventional MR imaging and histologic findings. *AJNR Am J Neuroradiol* 2001;22(5):969–976.
12. Borogovac A, Asllani I. Arterial spin labeling (ASL) fMRI: advantages, theoretical constraints, and experimental challenges in neurosciences. *Int J Biomed Imaging* 2012;2012:818456.
13. Cha S, Knopp EA, Johnson G, Wetzel SG, Litt AW, Zagzag D. Intracranial mass lesions: dynamic contrast-enhanced susceptibility-weighted echo-planar perfusion MR imaging. *Radiology* 2002;223(1):11–29.
14. Cha S. Perfusion MR imaging: basic principles and clinical applications. *Magn Reson Imaging Clin N Am* 2003;11(3):403–413.
15. Aronen HJ, Perkiö J. Dynamic susceptibility contrast MRI of gliomas. *Neuroimaging Clin N Am* 2002;12(4):501–523.
16. Thompson G, Mills SJ, Stivaros SM, Jackson A. Imaging of brain tumors: perfusion/permeability. *Neuroimaging Clin N Am* 2010;20(3):337–353.
17. Cha S, Tihan T, Crawford F, et al. Differentiation of low-grade oligodendroglomas from low-grade astrocytomas by using quantitative blood-volume measurements derived from dynamic susceptibility contrast-enhanced MR imaging. *AJNR Am J Neuroradiol* 2005;26(2):266–273.
18. Hartmann M, Heiland S, Harting I, et al. Differentiation of primary cerebral lymphoma from high-grade glioma with perfusion-weighted magnetic resonance imaging. *Neurosci Lett* 2003;338(2):119–122.
19. Liao W, Liu Y, Wang X, et al. Differentiation of primary central nervous system lymphoma and high-grade glioma with dynamic susceptibility contrast-enhanced perfusion magnetic resonance imaging. *Acta Radiol* 2009;50(2):217–225.
20. Filippi M, Rocca MA, De Stefano N, et al. Magnetic resonance techniques in multiple sclerosis: the present and the future. *Arch Neurol* 2011;68(12):1514–1520.
21. Ge Y, Law M, Johnson G, et al. Dynamic susceptibility contrast perfusion MR imaging of multiple sclerosis lesions: characterizing hemodynamic impairment and inflammatory activity. *AJNR Am J Neuroradiol* 2005;26(6):1539–1547.
22. Dowling C, Bollen AW, Noworolski SM, et al. Preoperative proton MR spectroscopic imaging of brain tumors: correlation with histopathologic analysis of resection specimens. *AJNR Am J Neuroradiol* 2001;22(4):604–612.
23. Hollingsworth W, Medina LS, Lenkinski RE, et al. A systematic literature review of magnetic resonance spectroscopy for the characterization of brain tumors. *AJNR Am J Neuroradiol* 2006;27(7):1404–1411.
24. Brandão LA, Shiroishi MS, Law M. Brain tumors: a multimodality approach with diffusion-weighted imaging, diffusion tensor imaging, magnetic resonance spectroscopy, dynamic susceptibility contrast and dynamic contrast-enhanced magnetic resonance imaging. *Magn Reson Imaging Clin N Am* 2013;21(2):199–239.
25. Bendszus M, Warmuth-Metz M, Klein R, et al. MR spectroscopy in gliomatosis cerebri. *AJNR Am J Neuroradiol* 2000;21(2):375–380.
26. Brandão L, Domingues R. Intracranial neoplasms. Philadelphia, Pa: Lippincott, Williams & Wilkins, 2002; 156–164.
27. Lai PH, Ho JT, Chen WL, et al. Brain abscess and necrotic brain tumor: discrimination with proton MR spectroscopy and diffusion-weighted imaging. *AJNR Am J Neuroradiol* 2002;23(8):1369–1377.
28. McGirt MJ, Chaichana KL, Gathinji M, et al. Independent association of extent of resection with survival in patients with malignant brain astrocytoma. *J Neurosurg* 2009;110(1):156–162.
29. Smith JS, Chang EF, Lamborn KR, et al. Role of extent of resection in the long-term outcome of low-grade hemispheric gliomas. *J Clin Oncol* 2008;26(8):1338–1345.
30. Garrett MC, Pouratian N, Liau LM. Use of language mapping to aid in resection of gliomas in eloquent brain regions. *Neurosurg Clin N Am* 2012;23(3):497–506.
31. Dimou S, Battisti RA, Hermens DF, Lagopoulos J. A systematic review of functional magnetic resonance imaging and diffusion tensor imaging modalities used in presurgical planning of brain tumour resection. *Neurosurg Rev* 2013;36(2):205–214; discussion 214.
32. Ogawa S, Lee TM, Nayak AS, Glynn P. Oxygenation-sensitive contrast in magnetic resonance image of rodent brain at high magnetic fields. *Magn Reson Med* 1990;14(1):68–78.
33. Logothetis NK. The underpinnings of the BOLD functional magnetic resonance imaging signal. *J Neurosci* 2003;23(10):3963–3971.
34. Huettel SA, Song AW, McCarthy G. Spatial and temporal properties of fMRI. In: Huettel SA, McCarthy G, eds. Functional magnetic resonance imaging. Sunderland, England: Sinauer, 2004; 185–216.
35. Goebel R. Localization of brain activity using functional magnetic resonance imaging. In: Stippich C, ed. Clinical functional MRI: presurgical functional neuroimaging. Heidelberg, Germany: Springer-Verlag, 2007; 9–51.
36. Kesavadas C, Thomas B, Sujesh S, et al. Real-time functional MR imaging (fMRI) for presurgical evaluation of paediatric epilepsy. *Pediatr Radiol* 2007;37(10):964–974.
37. Leach JL, Holland SK. Functional MRI in children: clinical and research applications. *Pediatr Radiol* 2010;40(1):31–49.
38. Lee MH, Smyser CD, Shimony JS. Resting-state fMRI: a review of methods and clinical applications. *AJNR Am J Neuroradiol* 2013;34(10):1866–1872.
39. Zhang D, Johnston JM, Fox MD, et al. Preoperative sensorimotor mapping in brain tumor patients using spontaneous fluctuations in neuronal activity imaged with functional magnetic resonance imaging: initial experience. *Neurosurgery* 2009;65(6 suppl):226–236.
40. Medina LS, Bernal B, Ruiz J. Role of functional MR in determining language dominance in epilepsy and nonepilepsy populations: a Bayesian analysis. *Radiology* 2007;242(1):94–100.
41. Bizzzi A, Blasi V, Falini A, et al. Presurgical functional MR imaging of language and motor functions: validation with intraoperative electrocortical mapping. *Radiology* 2008;248(2):579–589.
42. Giussani C, Roux FE, Ojemann J, Sganzerla EP, Pirillo D, Papagno C. Is preoperative functional

- magnetic resonance imaging reliable for language areas mapping in brain tumor surgery? review of language functional magnetic resonance imaging and direct cortical stimulation correlation studies. *Neurosurgery* 2010;66(1):113–120.
43. Kundu B, Penwarden A, Wood JM, et al. Association of functional magnetic resonance imaging indices with postoperative language outcomes in patients with primary brain tumors. *Neurosurg Focus* 2013;34(4):E6.
 44. Kapsalakis IZ, Kapsalaki EZ, Gotsis ED, et al. Preoperative evaluation with fMRI of patients with intracranial gliomas. *Radiol Res Pract* 2012;2012:727810.
 45. Lehéricy S, Duffau H, Cornu P, et al. Correspondence between functional magnetic resonance imaging somatotopy and individual brain anatomy of the central region: comparison with intraoperative stimulation in patients with brain tumors. *J Neurosurg* 2000;92(4):589–598.
 46. Li SW, Wang JF, Jiang T, et al. Preoperative 3T high field blood oxygen level dependent functional magnetic resonance imaging for glioma involving sensory cortical areas. *Chin Med J (Engl)* 2010;123(8):1006–1010.
 47. Roessler K, Donat M, Lanzenberger R, et al. Evaluation of preoperative high magnetic field motor functional MRI (3 Tesla) in glioma patients by navigated electrocortical stimulation and postoperative outcome. *J Neurol Neurosurg Psychiatry* 2005;76(8):1152–1157.
 48. Alexander AL, Lee JE, Lazar M, Field AS. Diffusion tensor imaging of the brain. *Neurotherapeutics* 2007;4(3):316–329.
 49. Mori S, van Zijl PC. Fiber tracking: principles and strategies—a technical review. *NMR Biomed* 2002;15(7–8):468–480.
 50. Nimsky C, Ganslandt O, Fahlbusch R. Implementation of fiber tract navigation. *Neurosurgery* 2007;61(1 suppl):306–317; discussion 317–318.
 51. Richter M, Zolal A, Ganslandt O, Buchfelder M, Nimsky C, Merhof D. Evaluation of diffusion-tensor imaging-based global search and tractography for tumor surgery close to the language system. *PLoS One* 2013;8(1):e50132.
 52. Bozzao A, Romano A, Angelini A, et al. Identification of the pyramidal tract by neuronavigation based on intraoperative magnetic resonance tractography: correlation with subcortical stimulation. *Eur Radiol* 2010;20(10):2475–2481.
 53. Berman JI, Berger MS, Chung SW, Nagarajan SS, Henry RG. Accuracy of diffusion tensor magnetic resonance imaging tractography assessed using intraoperative subcortical stimulation mapping and magnetic source imaging. *J Neurosurg* 2007;107(3):488–494.
 54. Ohue S, Kohno S, Inoue A, et al. Accuracy of diffusion tensor magnetic resonance imaging-based tractography for surgery of gliomas near the pyramidal tract: a significant correlation between subcortical electrical stimulation and postoperative tractography. *Neurosurgery* 2012;70(2):283–293; discussion 294.
 55. Wu JS, Zhou LF, Tang WJ, et al. Clinical evaluation and follow-up outcome of diffusion tensor imaging-based functional neuronavigation: a prospective, controlled study in patients with gliomas involving pyramidal tracts. *Neurosurgery* 2007;61(5):935–948; discussion 948–949.
 56. Kamada K, Todo T, Masutani Y, et al. Visualization of the frontotemporal language fibers by tractography combined with functional magnetic resonance imaging and magnetoencephalography. *J Neurosurg* 2007;106(1):90–98.
 57. Leclercq D, Duffau H, Delmaire C, et al. Comparison of diffusion tensor imaging tractography of language tracts and intraoperative subcortical stimulations. *J Neurosurg* 2010;112(3):503–511.
 58. Farquharson S, Tournier JD, Calamante F, et al. White matter fiber tractography: why we need to move beyond DTI. *J Neurosurg* 2013;118(6):1367–1377.
 59. Kuhnt D, Bauer MH, Egger J, et al. Fiber tractography based on diffusion tensor imaging compared with high-angular-resolution diffusion imaging with compressed sensing: initial experience. *Neurosurgery* 2013;72(suppl 1):165–175.
 60. Fernandez-Miranda JC, Pathak S, Engh J, et al. High-definition fiber tractography of the human brain: neuroanatomical validation and neurosurgical applications. *Neurosurgery* 2012;71(2):430–453.
 61. Price SJ. The role of advanced MR imaging in understanding brain tumour pathology. *Br J Neurosurg* 2007;21(6):562–575.
 62. Smits M, Vernooy MW, Wielopolski PA, Vincent AJ, Houston GC, van der Lugt A. Incorporating functional MR imaging into diffusion tensor tractography in the preoperative assessment of the corticospinal tract in patients with brain tumors. *AJR Am J Neuroradiol* 2007;28(7):1354–1361.
 63. McPherson CM, Leach JL, Vagal AV, et al. Operative integration of functional MRI and diffusion tensor tractography performed at 3T: correlation of resection extent and localization with post-operative clinical outcome in patients with brain neoplasia. Presented at the annual meeting of the Congress of Neurologic Surgeons, Orlando, Fla, September 20–25, 2008.
 64. Bohinski RJ, Warnick RE, Gaskill-Shipley MF, et al. Intraoperative magnetic resonance imaging to determine the extent of resection of pituitary macroadenomas during transsphenoidal microsurgery. *Neurosurgery* 2001;49(5):1133–1143; discussion 1143–1144.
 65. Senft C, Bink A, Franz K, Vatter H, Gasser T, Seifert V. Intraoperative MRI guidance and extent of resection in glioma surgery: a randomised, controlled trial. *Lancet Oncol* 2011;12(11):997–1003.
 66. Bohinski RJ, Kokkino AK, Warnick RE, et al. Glioma resection in a shared-resource magnetic resonance operating room after optimal image-guided frameless stereotactic resection. *Neurosurgery* 2001;48(4):731–742; discussion 742–744.
 67. Kelly PJ, Daumas-Dupont C, Kispert DB, Kall BA, Scheithauer BW, Illig JJ. Imaging-based stereotaxic serial biopsies in untreated intracranial glial neoplasms. *J Neurosurg* 1987;66(6):865–874.
 68. Guarascelli J, Vagal A, McKenzie J, et al. Target definition for malignant gliomas: no difference in radiation treatment volumes between 1.5T and 3T magnetic resonance imaging. Presented at the annual meeting of ASTRO, Miami, Fla, October 2–6, 2011.
 69. Krishnan AP, Asher IM, Davis D, Okunieff P, O'Dell WG. Evidence that MR diffusion tensor imaging (tractography) predicts the natural history of regional progression in patients irradiated conformally for primary brain tumors. *Int J Radiat Oncol Biol Phys* 2008;71(5):1553–1562.

70. Mammar H, Kerrou K, Nataf V, et al. Positron emission tomography/computed tomography imaging of residual skull base chordoma before radiotherapy using fluoromisonidazole and fluorodeoxyglucose: potential consequences for dose painting. *Int J Radiat Oncol Biol Phys* 2012;84(3):681–687.
71. Oser AB, Moran CJ, Kaufman BA, Park TS. Intracranial tumor in children: MR imaging findings within 24 hours of craniotomy. *Radiology* 1997;205(3):807–812.
72. Winterstein M, Münter MW, Burkholder I, Essig M, Kauczor HU, Weber MA. Partially resected gliomas: diagnostic performance of fluid-attenuated inversion recovery MR imaging for detection of progression. *Radiology* 2010;254(3):907–916.
73. Hamstra DA, Chenevert TL, Moffat BA, et al. Evaluation of the functional diffusion map as an early biomarker of time-to-progression and overall survival in high-grade glioma. *Proc Natl Acad Sci U S A* 2005;102(46):16759–16764.
74. Hein PA, Eskey CJ, Dunn JF, Hug EB. Diffusion-weighted imaging in the follow-up of treated high-grade gliomas: tumor recurrence versus radiation injury. *AJNR Am J Neuroradiol* 2004;25(2):201–209.
75. Asao C, Korogi Y, Kitajima M, et al. Diffusion-weighted imaging of radiation-induced brain injury for differentiation from tumor recurrence. *AJNR Am J Neuroradiol* 2005;26(6):1455–1460.
76. Clarke JL, Chang S. Pseudoprogression and pseudoresponse: challenges in brain tumor imaging. *Curr Neurol Neurosci Rep* 2009;9(3):241–246.
77. Jain R, Narang J, Sundgren PM, et al. Treatment induced necrosis versus recurrent/progressing brain tumor: going beyond the boundaries of conventional morphologic imaging. *J Neurooncol* 2010;100(1):17–29.
78. Fink J, Born D, Chamberlain MC. Radiation necrosis: relevance with respect to treatment of primary and secondary brain tumors. *Curr Neurol Neurosci Rep* 2012;12(3):276–285.
79. Siu A, Wind JJ, Iorgulescu JB, Chan TA, Yamada Y, Sherman JH. Radiation necrosis following treatment of high grade gliomas: a review of the literature and current understanding. *Acta Neurochir (Wien)* 2012;154(2):191–201; discussion 201.
80. Fatterpekar GM, Galheigo D, Narayana A, Johnson G, Knopp E. Treatment-related change versus tumor recurrence in high-grade gliomas: a diagnostic conundrum—use of dynamic susceptibility contrast-enhanced (DSC) perfusion MRI. *AJR Am J Roentgenol* 2012;198(1):19–26.
81. Barajas RF Jr, Chang JS, Segal MR, et al. Differentiation of recurrent glioblastoma multiforme from radiation necrosis after external beam radiation therapy with dynamic susceptibility-weighted contrast-enhanced perfusion MR imaging. *Radiology* 2009;253(2):486–496.
82. Rock JP, Hearshen D, Scarpace L, et al. Correlations between magnetic resonance spectroscopy and image-guided histopathology, with special attention to radiation necrosis. *Neurosurgery* 2002;51(4):912–919; discussion 919–920.
83. Chamberlain MC, Glantz MJ, Chalmers L, Van Horn A, Sloan AE. Early necrosis following concurrent Temodar and radiotherapy in patients with glioblastoma. *J Neurooncol* 2007;82(1):81–83.
84. Brandes AA, Tosoni A, Spagnolli F, et al. Disease progression or pseudoprogression after concomitant radiochemotherapy treatment: pitfalls in neurooncology. *Neuro Oncol* 2008;10(3):361–367.
85. Taal W, Brandsma D, de Bruin HG, et al. Incidence of early pseudo-progression in a cohort of malignant glioma patients treated with chemoirradiation with temozolamide. *Cancer* 2008;113(2):405–410.
86. Brandsma D, Stalpers L, Taal W, Sminia P, van den Bent MJ. Clinical features, mechanisms, and management of pseudoprogression in malignant gliomas. *Lancet Oncol* 2008;9(5):453–461.
87. Mangla R, Singh G, Ziegelitz D, et al. Changes in relative cerebral blood volume 1 month after radiation-temozolomide therapy can help predict overall survival in patients with glioblastoma. *Radiology* 2010;256(2):575–584.
88. Santra A, Kumar R, Sharma P, et al. F-18 FDG PET-CT in patients with recurrent glioma: comparison with contrast enhanced MRI. *Eur J Radiol* 2012;81(3):508–513.

Critical Role of Imaging in the Neurosurgical and Radiotherapeutic Management of Brain Tumors

Lily L. Wang, MBBS, MPH • James L. Leach, MD • John C. Breneman, MD • Christopher M. McPherson, MD • Mary F. Gaskill-Shipley, MD

RadioGraphics 2014; 34:702–721 • Published online 10.1148/rg.343130156 • Content Codes: **CT** **MR** **NR** **OI**

Page 704

Compared with GBM, lymphomas typically have lower relative CBV ratios due to differences in tumor vascularity. Although it is not a specific finding, lymphomas often demonstrate increased signal relative to baseline in the recovery phase due to contrast material leakage within the interstitial space.

Page 709

Functional MR imaging and DTI-based tractography have become useful tools in preoperative assessment and imaging-guided surgical therapy in patients with brain tumors in or near eloquent brain regions.

Page 712

If clinically feasible, postoperative imaging should be performed within the first 24 hours. Although mild reactive enhancement can be present immediately after surgery, nodular or masslike enhancement seen within 24 hours typically represents residual tumor.

Page 714

[C]omparison of new areas of enhancement with areas of restricted diffusion seen at immediate postoperative imaging is important. If these areas match, the enhancement most likely represents reactive changes or subacute enhancing ischemia rather than recurrent tumor.

Page 714–715

If a new or enlarged area of signal abnormality and restricted diffusion is seen in a postoperative margin that previously had demonstrated no restricted diffusion, tumor recurrence is likely.